

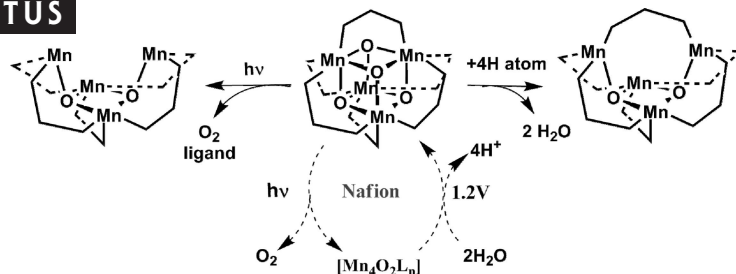
## Development of Bioinspired $\text{Mn}_4\text{O}_4$ —Cubane Water Oxidation Catalysts: Lessons from Photosynthesis

G. CHARLES DISMUKES,<sup>\*,†</sup> ROBIN BRIMBLECOMBE,<sup>‡,§</sup>  
 GREG A. N. FELTON,<sup>§</sup> RUSLAN S. PRYADUN,<sup>§</sup>  
 JOHN E. SHEATS,<sup>§</sup> LEONE SPICCIA,<sup>‡</sup> AND  
 GERHARD F. SWIEGERS<sup>⊥</sup>

<sup>†</sup>Department of Chemistry & Chemical Biology, Waksman Institute, Rutgers University, Piscataway, New Jersey 08854, <sup>‡</sup>School of Chemistry, Monash University, Wellington Road, Clayton, Victoria 3800, Australia, <sup>§</sup>Department of Chemistry, Princeton University, Princeton, New Jersey 08540, <sup>⊥</sup>Intelligent Polymer Research Institute, University of Wollongong, Wollongong, New South Wales 2522, Australia

RECEIVED ON SEPTEMBER 23, 2009

### CON SPECTUS



Hydrogen is the most promising fuel of the future owing to its carbon-free, high-energy content and potential to be efficiently converted into either electrical or thermal energy. The greatest technical barrier to accessing this renewable resource remains the inability to create inexpensive catalysts for the solar-driven oxidation of water. To date, the most efficient system that uses solar energy to oxidize water is the photosystem II water-oxidizing complex (PSII-WOC), which is found within naturally occurring photosynthetic organisms. The catalytic core of this enzyme is a  $\text{CaMn}_4\text{O}_x$  cluster, which is present in all known species of oxygenic phototrophs and has been conserved since the emergence of this type of photosynthesis about 2.5 billion years ago. The key features that facilitate the catalytic success of the PSII-WOC offer important lessons for the design of abiological water oxidation catalysts.

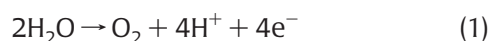
In this Account, we examine the chemical principles that may govern the PSII-WOC by comparing the water oxidation capabilities of structurally related synthetic manganese-oxo complexes, particularly those with a cubical  $\text{Mn}_4\text{O}_4$  core (“cubanes”). We summarize this research, from the self-assembly of the first such clusters, through the elucidation of their mechanism of photoinduced rearrangement to release  $\text{O}_2$ , to recent advances highlighting their capability to catalyze sustained light-activated electrolysis of water.

The  $[\text{Mn}_4\text{O}_4]^{6+}$  cubane core assembles spontaneously in solution from monomeric precursors or from  $[\text{Mn}_2\text{O}_2]^{3+}$  core complexes in the presence of metrically appropriate bidentate chelates, for example, diarylphosphinates (ligands of  $\text{Ph}_2\text{PO}_2^-$  and 4-phenyl-substituted derivatives), which bridge pairs of Mn atoms on each cube face ( $\text{Mn}_4\text{O}_4\text{L}_6$ ). The  $[\text{Mn}_4\text{O}_4]^{6+}$  core is enlarged relative to the  $[\text{Mn}_2\text{O}_2]^{3+}$  core, resulting in considerably weaker Mn—O bonds. Cubanes are ferocious oxidizing agents, stronger than analogous complexes with the  $[\text{Mn}_2\text{O}_2]^{3+}$  core, as demonstrated both by the range of substrates they dehydrogenate or oxygenate (unactivated alkanes, for example) and the 25% larger O—H bond enthalpy of the resulting  $\mu_3$ -OH bridge.

The cubane core topology is structurally suited to releasing  $\text{O}_2$ , and it does so in high yield upon removal of one phosphinate by photoexcitation in the gas phase or thermal excitation in the solid state. This is quite unlike other Mn-oxo complexes and can be attributed to the elongated Mn—O bond lengths and low-energy transition state to the  $\mu$ -peroxo precursor. The photoproduct,  $[\text{Mn}_4\text{O}_2\text{L}_5]^+$ , an intact nonplanar butterfly core complex, is poised for oxidative regeneration of the cubane core upon binding of two water molecules and coupling to an anode. Catalytic evolution of  $\text{O}_2$  and protons from water exceeding 1000 turnovers can be readily achieved by suspending the oxidized cubane,  $[\text{Mn}_4\text{O}_4\text{L}_6]^+$ , into a proton-conducting membrane (Nafion) preadsorbed onto a conducting electrode and electrooxidizing the photoreduced butterfly complexes by the application of an external bias. Catalytic water oxidation can be achieved using sunlight as the only source of energy by replacing the external electrical bias with redox coupling to a photoanode incorporating a Ru(bipyridyl) dye.

## Introduction

The need to replace finite fossil fuels with abundant, renewable, environmentally friendly energy sources is both pressing and globally recognized. One long-sought solution is the development of a photoelectrochemical device in which sunlight efficiently splits water into oxygen, O<sub>2</sub>, at the anode and hydrogen, H<sub>2</sub>, at the cathode.<sup>1,2</sup> The key technical impediment to such a cell is the need for and present-day absence of efficient, low-cost catalysts capable of oxidizing water using sunlight to drive this energetically highly unfavorable reaction ( $\Delta H^\circ = 572$  kJ/mol):



The equivalent uncatalyzed atomic dissociation reaction requires a temperature of 2500 °C to break the four strong O–H bonds (enthalpy  $\Delta H^\circ = 494$  kJ/mol each).<sup>3</sup> The energy barrier can be significantly lowered by coupling the dissociation steps to the energy-releasing step of O–O bond formation ( $\Delta H^\circ = -494$  kJ/mol). This can, however, only occur via the intermediacy of a catalyst that is constrained to rearrange these five bonds in a coordinated sequence with picometer precision and without releasing reactive intermediates. Delivering the necessary energy input into these bonds while overcoming the mechanistic complexity is among the “Holy Grails” of chemistry.<sup>1,2</sup>

In this Account, we describe the chemical principles that Nature appears to use to catalyze water oxidation by photosynthesis<sup>4–6</sup> by highlighting one particular class of manganese–oxo clusters that adopt these attributes: (i) cluster self-assembly, repair, and flexibility; (ii) constrained Mn oxidation states; (iii) mobility of protons and their coupling to electron transport; and (iv) mechanistic requirements for dioxygen bond formation and turnover.

The active site of the photosystem II water-oxidizing complex (PSII-WOC) within oxygenic phototrophs comprises a CaMn<sub>4</sub>O<sub>x</sub> core; the stoichiometry is based upon electron paramagnetic resonance (EPR) and extended X-ray absorption fine structure (EXAFS) experiments<sup>5</sup> and reconstitution of the cluster from its elemental constituents.<sup>7</sup> This core composition is conserved in all photosynthetic organisms and thus appears to be the sole biological innovation that can do this chemistry. Five oxidation states are produced following four successive light flashes differing by one electron each, denoted S<sub>0</sub>, S<sub>1</sub>, ..., S<sub>4</sub>. The PSII-WOC turnover rate in whole cells of live microalgae is typically  $(1-4) \times 10^2$  s<sup>-1</sup> and  $10^3$  s<sup>-1</sup> *in vitro*.

Early EPR and EXAFS experiments identified eight possible Mn<sub>4</sub>O<sub>x</sub> topologies,<sup>8–10</sup> which were narrowed to two to three core types by subsequent XRD of single crystals of a cyanobacterial PSII-WOC in the resting S<sub>1</sub> state. The precise

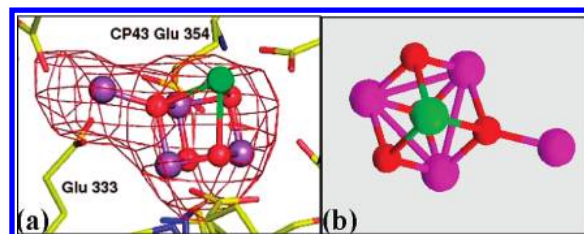


**FIGURE 1.** XRD model of the Mn<sub>4</sub>Ca core of cyanobacterial PSII-WOC according to (a) Ferreira et al.<sup>6,15</sup> and (b) Guskov et al.<sup>13</sup> Reprinted with permission from ref 13. Copyright 2009 Wiley-VCH Verlag GmbH & Co. KGaA. Ca (green), O (red) Mn (purple).

connectivity of the core has been debated owing to limited resolution and radiation-induced reduction or damage.<sup>11</sup> However, the early model<sup>12</sup> of a three plus one organization of the four Mn atoms has remained in the more recent structures determined by higher resolution (2.9–3.5 Å) X-ray diffraction (XRD)<sup>6,13</sup> and polarized single-crystal Mn-EXAFS.<sup>14</sup> All of these models contain a plane of three Mn atoms forming an approximate equilateral triangle with the Ca atom located above the plane positioned either on the 3-fold axis defined by the three Mn atoms (trigonal pyramid or C<sub>3v</sub> symmetry, Figure 1)<sup>6,13,15</sup> or displaced slightly off the 3-fold axis within one of the three perpendicular planes (C<sub>2v</sub> symmetry).<sup>14</sup> The distances between the three Mn and Ca are compatible with the presence of bridging oxygen atoms (O, OH, or OH<sub>2</sub>). Although the “oxos” are not distinguishable at present resolution, the C<sub>3v</sub> and C<sub>2v</sub> models suggest these “oxos” are either chemically equivalent (C<sub>3v</sub>) or a mixture of these three types (C<sub>2v</sub>) in the resting S<sub>1</sub> oxidation state. The trigonal pyramidal CaMn<sub>3</sub> subcluster with four equivalent oxo bridges is depicted in Figure 1 from the XRD reports. We refer to this as the CaMn<sub>3</sub>O<sub>4</sub> *heterocubane* core type or its C<sub>2v</sub>-distorted counterpart as a CaMn<sub>3</sub>O<sub>x</sub> *distorted (or incomplete) heterocubane*. The fourth “dangler” Mn atom is fully coupled electronically to the heterocubane subcluster, probably via one<sup>6,15</sup> or two<sup>14</sup> “oxo” bridges. It is located in the same plane as the three Mn according to XRD models<sup>6,13,15</sup> or possibly out of this plane in one of the three Mn-EXAFS models.<sup>14</sup> From this, we conclude that there is substantial agreement identifying the WOC core as a CaMn<sub>3</sub>O<sub>x</sub> heterocubane subcluster plus tightly coupled dangler Mn. This topology has been further supported by high-level computational modeling of the core and side chains.<sup>16</sup>

With this model of the PSII-WOC in hand, we next consider synthetic Mn–oxo models, particularly those having the basic M<sub>4</sub>O<sub>4</sub> “cubane” topology, and examine their activity as water oxidation catalysts.

An early proposal for photosynthetic O<sub>2</sub> production involved a Mn<sub>4</sub>O<sub>4</sub> cube to Mn<sub>4</sub>O<sub>2</sub> butterfly rearrangement, but because there were no Mn<sub>4</sub>O<sub>4</sub> cube examples, it remained untested.<sup>17</sup> There are now over 100 structures of tetranuclear

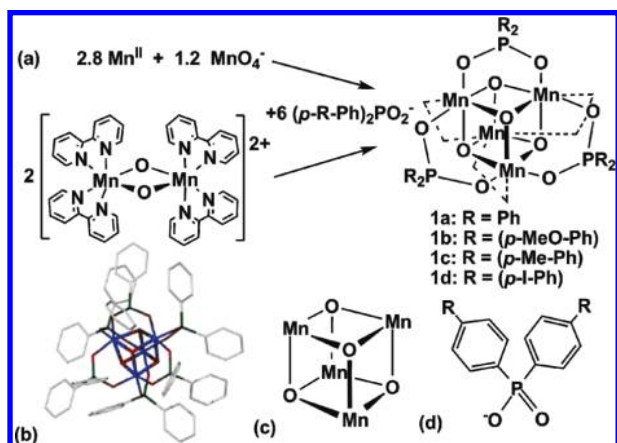


**FIGURE 2.** (a) Synthetic routes to  $\text{Mn}_4\text{O}_4\text{L}_6$  by self-assembly of preformed dimers (**1a–d**) or from  $\text{Mn}^{\text{II}}$  and  $\text{MnO}_4^-$  ions (**1a**),<sup>18,19</sup> (b) X-ray crystal structure of **1a** ( $\text{L}_6\text{Mn}_4\text{O}_4$ ,  $\text{L} = \text{Ph}_2\text{PO}_2^-$ ),<sup>19</sup> (c)  $[\text{Mn}_4\text{O}_4]$  cubane core, and (d) phosphinate ligand.

$\text{Mn}$ –oxo complexes in the CCDC database containing either cube-like  $\text{M}_4(\text{OX})_4$  cores, unsymmetrical (incomplete) cube-like cores, or the planar butterfly core  $[\text{Mn}_4\text{O}_2]^{n+}$ . Among these complexes, the first all oxo-bridged  $\text{Mn}_4\text{O}_4$  core complexes were  $[\text{Mn}_4\text{O}_4\text{L}_6]$ , **1a–d** (Figure 2, where  $\text{L}^- = (p\text{-R-C}_6\text{H}_4)_2\text{PO}_2^-$ ,  $\text{R} = \text{H}$  (**1a**),  $\text{OMe}$  (**1b**),  $\text{Me}$  (**1c**),  $\text{I}$  (**1d**)).<sup>18–21</sup> These molecules, denoted *cubanes*, are chelated by six facially capping phosphinates.

The feasibility of synthesis of a molecular complex containing the  $\text{CaMn}_3\text{O}_4$  heterocubane subcluster has been implicated indirectly, because this core type has been synthesized within a larger  $\text{Mn}_{13}$  cluster.<sup>22</sup> To date, no reactivity studies have been reported on this molecule.

## Self-Assembly and Flexibility

A water oxidation catalyst must take up two water molecules and transform them through various reactive intermediates into dioxygen and four free protons. This undoubtedly requires an ability to dynamically reform itself upon completion of the cycle. EPR and EXAFS experiments indicate that ligand coordination changes occur to  $\text{Mn}$  during light-induced cycling of the PSII-WOC.<sup>23</sup> The dark resting state of the  $\text{CaMn}_4\text{O}_x$  core in isolated PSII-WOC complexes is unstable and requires elevated levels of free  $\text{Ca}^{2+}$ ,  $\text{Cl}^-$ , and osmolyte to maintain the stability of the cofactors and protein conformation. The PSII-WOC protein provides a flexible, low coordination number environment for the  $\text{Mn}$  and  $\text{Ca}$  ions. The  $\text{CaMn}_4\text{O}_x$  core assembles spontaneously from the apo-WOC-PSII protein complex in the presence of light and the free cofactors.<sup>24</sup> The binding and photooxidation of  $\text{Mn}^{2+}$  occurs sequentially in the sequence  $1(h\nu) + \text{Ca}(\text{dark slow}) + 3(h\nu)$ . Calcium binding templates the protein for the rapid highly cooperative uptake of the last three  $\text{Mn}^{2+}$ . This suggests that it controls the formation and bonding stability of a

$\text{CaMn}_3$  unit. The similarity to the  $\text{CaMn}_3\text{O}_x$  heterocubane subcluster should be noted.

Thus, the first feature of a successful PSII water oxidation catalyst is likely to be ligand-guided self-assembly that retains coordination flexibility throughout the catalytic cycle. This feature is observed in several abiological  $\text{O}_2$ -evolving species.<sup>25</sup> For example, the  $\text{Mn}_4\text{O}_4\text{L}_6$  cubanes ( $\text{L} = \text{Ph}_2\text{PO}_2^-$ , **1a**) form by self-assembly starting from mononuclear precursors<sup>18</sup> or from two  $[\text{Mn}_2\text{O}_2]^{3+}$  core complexes in the presence of diphenylphosphinate ligands (Figure 2).<sup>19</sup> The reaction is driven in part by the formation of 12 interligand nonbonded associations ( $\pi$ – $\pi$  interactions) between the phenyl groups, as revealed in the XRD structure. All isolated derivatives thus far have diphenyl rings, confirming the role of phenyl packing for formation.

The high charge density of the  $[\text{Mn}_4\text{O}_4]^{6+}$  core and anticipated weaker bonding arising from the orthogonal bonds compared with planar oxo core types led us to predict that the core would be expanded, which was confirmed by XRD.<sup>19,26</sup> The  $\text{Mn}$ – $\text{Mn}$  separation in **1a** (2.95–3.0 Å) is 10–15% longer compared with that in  $[\text{Mn}_2\text{O}_2]^{3+}$  core complexes. Thus, the choice of phosphinate as capping ligand with its long interoxygen separation (2.58 Å) is crucial to forming **1a–d** in high yield. Carboxylates have a shorter bite distance ( $\text{O} \cdots \text{O} = 2.22$  Å) and cannot bridge the  $\text{Mn}$  atoms in the same way and do not form  $\text{Mn}_4\text{O}_4$  cubanes.<sup>19</sup>

Once formed, the cubical core is capable of phosphinate exchange in solution. This kinetic lability of the ligands facilitates attachment to phosphinate-functionalized surfaces. For example, bis(*p*-iodophenyl) phosphinate attaches to gold surfaces and allows exchange of cubanes onto the surface.<sup>21</sup> By contrast, the more acidic organosulfonates ( $\text{RSO}_3^-$ ) do not undergo ligand exchange in solution with phosphinate ligands on cubanes.

## Access to High Valence States

EPR and X-ray absorption near edge structure (XANES) experiments have identified  $\text{Mn}^{\text{III}}$  and  $\text{Mn}^{\text{IV}}$  oxidation states in each S-state of the catalytic cycle. Some mechanisms also propose a  $\text{Mn}^{\text{V}}$  oxidation state in  $\text{S}_4$ , although no experimental evidence supports this to date.<sup>27</sup>  $\text{Mn}^{\text{II}}$  has not yet been conclusively identified in any S-state of the cycle and has been excluded based on  $^{55}\text{Mn}$  electron nuclear double resonance (ENDOR),<sup>28</sup> although the possibility of one  $\text{Mn}^{\text{II}}$  in  $\text{S}_0$  remains an open question that is debated.<sup>8,29</sup> The electrochemical potentials of the PSII-WOC cluster vary throughout the S-state cycle in a narrow window,<sup>4</sup> and all are less than the electrochemical potential of the photooxidant pigment P680 (1.25 V



vs SHE).<sup>30</sup> Thus, the mean overpotential for water oxidation at pH 7 (0.82 V) is 0.43 V.

The redox potentials of Mn ions are determined by the ligand coordination number and ligand type, which determines electron donation (covalency) and proton ionization capacities.<sup>31</sup> In the CaMn<sub>3</sub> subcluster of the PSII-WOC, the adjustable ligand field is achieved by ionization of water molecules (yielding OH<sup>-</sup>, O<sup>2-</sup>) and protein residues coordinating Mn ions. Additional electrostatic and charge transfer interactions among the Mn and Ca ions are important in setting the absolute redox potentials of the S-states. These contributions are sufficient to achieve all of the Mn valence states required to oxidize water at a relatively constant potential.

In the cubane clusters **1a–d**, three oxo ligands and three phosphinate oxygen donors support each metal center, providing a strong ligand field. This facilitates the oxidation from  $2\text{Mn}^{\text{III}}2\text{Mn}^{\text{IV}}$  to  $\text{Mn}^{\text{III}}3\text{Mn}^{\text{IV}}$  at an electrochemical potential of 1.1 V (**1a**) and 0.94 V (**1b**) vs SHE, generating the  $[\text{Mn}_4\text{O}_4]^{7+}$  core.<sup>32</sup> The respective products **1a**<sup>+</sup> and **1b**<sup>+</sup> have been isolated and characterized as described below. The redox potential of the cubane core can be tuned by varying the functional groups on the phosphinate ligands and by protonation. For example, addition of 12 *p*-methoxy groups (**1b**) lowers the potential of the  $2\text{Mn}^{\text{III}}2\text{Mn}^{\text{IV}} \rightarrow \text{Mn}^{\text{III}}3\text{Mn}^{\text{IV}}$  transition by 0.15 V relative to the phenyl derivative (**1a**).<sup>26</sup>

Cubanes **1a–c** react with strong acids and O<sub>2</sub> to form the oxidized cubane [Mn<sub>4</sub>O<sub>4</sub>L<sub>6</sub>]<sup>+</sup>, **1a**<sup>+</sup>, **1b**<sup>+</sup>, and **1c**<sup>+</sup>, respectively.<sup>26,33</sup> This reaction occurs by protonation of an oxo, resulting in the release of a water molecule generating the incomplete cubane, [Mn<sub>4</sub>O<sub>3</sub>L<sub>6</sub>]<sup>+</sup>, which subsequently reacts with O<sub>2</sub> in air to form **1**<sup>+</sup> in essentially stoichiometric yield. This important reaction demonstrates a pathway for interconversion of water and O<sub>2</sub> via the μ<sub>3</sub>-oxo site. It is unique to the Mn–oxo cubanes.

X-ray crystal structures and EPR spectroscopy reveal that the  $[\text{Mn}_4\text{O}_4]^{7+}$  core is made up of  $1\text{Mn}^{\text{III}}3\text{Mn}^{\text{IV}}$ , which is the highest oxidation state observed in the cubane series.<sup>26,33</sup> It is interesting to note that this oxidation state is the observed precursor to catalytic  $\text{O}_2$  production from water by cubanes (see below). This oxidation state is equivalent to that claimed for the  $\text{S}_2$  state of the PSII-WOC based on XANES,<sup>10,23,34</sup> some EPR data,<sup>10,23</sup> and Mn-ENDOR<sup>28</sup> or to the  $\text{S}_4$  ( $\text{O}_2$ -evolving) state in other interpretations.<sup>8,29</sup>

Between the  $\text{Mn}_4\text{O}_4$  cubane and  $\text{Mn}_4\text{O}_2$  butterfly series of core types, five redox states have been observed that contain  $\text{Mn}^{\text{II}}$ ,  $\text{Mn}^{\text{III}}$ , and  $\text{Mn}^{\text{IV}}$  oxidation states. By contrast, all dimanganese complexes, which cycle through five redox states, must form at least four Mn oxidation states (Mn-centered). Therefore, the redox leveling requirements demanded

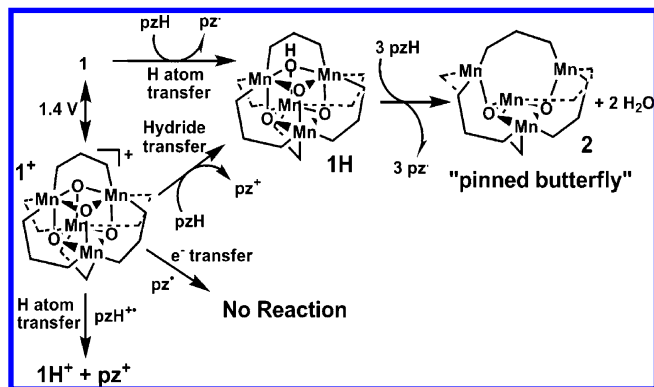


**FIGURE 3.** PCET reactions of the cubane model complexes  $\text{Mn}_4\text{O}_4\text{L}_6$ , **1a** and **1a**<sup>+</sup> ( $\text{L}^- = (\text{C}_6\text{H}_5)_2\text{PO}_2^-$ ).<sup>37,38</sup>

of a dimanganese catalyst to cycle through four or more redox states using a fixed potential oxidant are considerably more difficult to achieve.

## Proton-Coupled Electron Transfer (PCET)

An essential feature of the PSII-WOC that allows it to oxidize water at a low overpotential is its ability to utilize *proton-coupled electron transfer* reactions (PCET) to lower the energetic cost of independent proton and electron ionization reactions.<sup>27,35</sup> As an example, if water oxidation were to formally involve a one  $e^-$  oxidation step it would cost a prohibitively high energy (IP = 1220 kJ mol<sup>-1</sup> in the gas phase). This barrier may be circumvented by combining electron and proton transfer steps by PCET, to achieve the H–OH bond dissociation energy (BDE = 500 kJ mol<sup>-1</sup> in the gas phase) for a net H atom loss. The BDE is further diminished by binding the  $e^-/H^+$  and the OH• intermediates to suitable sites within the catalyst.<sup>36</sup>

The cubanes illustrate the importance of PCET in their redox reactions with H atom donors. For example, **1a**<sup>+</sup> reacts sequentially with amines like phenothiazine (pzhH), consuming a total of four H<sup>+</sup> and five e<sup>-</sup>.<sup>37,38</sup> The products, observed by electrospray mass spectrometry and Fourier-transform infrared (FTIR) spectroscopy, are two water molecules derived from the corner oxos and the deoxygenated cluster, Mn<sub>4</sub>O<sub>2</sub>L<sub>6</sub>, called the “pinned butterfly” **2a** (Figure 3).<sup>37,38</sup> The pinned butterfly species has Mn oxidation states of 2Mn<sup>II</sup>2Mn<sup>III</sup>, determined by EPR spectroscopy. Its solution structure is based on evidence obtained via multiple spectroscopic techniques (EPR, NMR, ESI-MS, FTIR). Four sequentially formed hydrogenated intermediates were observed,<sup>38</sup> and one of these, **1a-H**, was isolated and characterized.<sup>37</sup> Isolation of the next hydrogenated intermediate, **1a-2H**, was prevented by release of a water molecule, but the corresponding methanolysis product of **1b-2H**, [Mn<sub>4</sub>O<sub>4</sub>(μ-OMe)<sub>2</sub>(MeOPh)<sub>2</sub>PO<sub>2</sub>]<sub>6</sub>(HOMe)], has been isolated and characterized.<sup>39</sup>

The energetic requirement for PCET for each reduction step is demonstrated by the reaction of  $\text{pzH}^+$  (the radical cation) with cubium **1a**<sup>+</sup> by H atom transfer to produce the  $\text{pz}^+$  cation and **1a-H**<sup>•</sup>.<sup>37</sup> By contrast, the  $\text{pz}^{\bullet}$  radical does not reduce **1a**<sup>+</sup> by electron transfer because it is energetically unfavorable without the added driving force of protonation at an oxo (Figure 3).<sup>37</sup> This observation has direct relevance to the PSII-WOC where the energetic constraints of electron-only oxidation by a chlorophyll radical with fixed potential (P680) are alleviated by the coupling of proton release with electron extraction during S-state transitions.<sup>35,36</sup>

The O–H bond dissociation enthalpy (BDE) of the  $\mu_3$ -OH in **1a-H** was estimated using a standard thermodynamic cycle and calibration against six known BDEs for its reaction partners.<sup>40</sup> The resulting O–H BDE of **1a-H** (Figure 3) was greater than all of the standards ( $>394 \text{ kJ mol}^{-1}$ ).<sup>36,37</sup> Comparing this to the much weaker mean  $\mu_2$ -OH BDE of multiple complexes containing the  $[\text{Mn}_2\text{O}(\text{OH})]^{3+}$  core (320 kJ/mol) reveals that the O–H bond in the  $[\text{Mn}_4\text{O}_3(\text{OH})]^{6+}$  core of **1a-H** is substantially stronger ( $>20\%$ ). This difference is attributable to the longer (weaker) Mn–O bonds of the cubane core. The strong O–H bond in **1a-H** explains the potent oxidizing capacity of **1a-c**, which abstracts H atoms from unactivated alkanes, as well as the oxidation of thioesters, alkenes, alcohols, and aldehydes.<sup>18,39</sup>

Using a method developed by Parker and co-workers<sup>41</sup> and applied to Mn complexes by Mayer and co-workers,<sup>42</sup> we determined the free energy for the dissociation of hydride ( $\text{H}^-$ ) from **1a-H** (**3**) to be greater than 530 kJ/mol.<sup>37</sup> This observation demonstrates that the  $[\text{Mn}_4\text{O}_4]^{7+}$  core of **1a**<sup>+</sup> is a ferocious oxidant capable of concerted  $2\text{e}^-/1\text{H}^+$  PCET chemistry. It is of direct relevance to the energetically favored two-electron pathway for PSII-WOC mediated water oxidation predicted by Kristalik.<sup>36</sup>

## O–O Bond Formation and $\text{O}_2$ Release

Although the exact mechanism of dioxygen formation and release by PSII-WOC is still uncertain, some constraints clearly exist.<sup>36,43</sup> There is no direct evidence for a terminal oxo ( $\text{Mn}=\text{O}$ ) or bound peroxide intermediate in any S-state.<sup>8</sup>  $\text{O}_2$  release is spontaneous upon forming the O–O bond in  $\text{S}_4$  and is preceded by proton release.<sup>27</sup>  $\text{Ca}^{2+}$  participates in forming the O–O bond and  $\text{O}_2$  release in the rate-limiting step of the last ( $\text{S}_3 \rightarrow \text{S}_0$ ) transition.<sup>8,36</sup> This reaction is irreversible. A feature of the enzyme that appears to be essential for O–O bond formation is the flexible coordination number and nondirectional bonding required at the calcium effector site. The dynamic nature of the calcium site is also evident by its role in ionization of water molecules that form the oxo bridges to

Mn ions during *de novo* biogenesis and repair of the fully assembled  $\text{CaMn}_4\text{O}_x$  core, a process known as photoactivation.<sup>44</sup> Alternative interpretations of the role of calcium emphasize its properties as a weak Lewis acid. One proposal suggests it could serve to ionize a bound water molecule to form a nucleophilic hydroxide.<sup>45</sup>

As in the PSII-WOC, the formation of dioxygen in the cubane system is limited by an activation barrier.<sup>8</sup> Lacking the flexibility of a Ca ion that has no directional bonding preference and thus enables formation of a bridging peroxo,  $\text{Ca}(\mu\text{-O}_2)\text{Mn}$ , the Mn centers in the cubane are restricted by their orthogonal d-orbital bonding and thus form relatively rigid (directional) ligand bonds.<sup>36</sup> These restrict the flexibility of the core and impose a barrier to  $\text{O}_2$  release. However, in the gas phase the large kinetic barrier can be lowered by removal of one of the capping phosphinate ligands, thereby providing sufficient flexibility in the core to allow O–O bond formation and release.<sup>46</sup>

The gas-phase photochemistry of **1a-c** and **(1a-c)**<sup>+</sup> proves unequivocally the preference for selective  $\text{O}_2$  release from the cubane cores and its absence for complexes containing the  $[\text{Mn}_2\text{O}_2]^{3+/4+}$  cores.<sup>20,26,46</sup> Matrix-free laser desorption/ionization time-of-flight mass spectrometry (LDI-MS-TOF) was used to detect products formed by laser excitation at 337 nm (excites a Mn–O charge transfer band). The resulting positive ion spectrum of **1a** consists of only two products at all laser powers investigated: the parent cation **1a**<sup>+</sup>, and the photoproduct,  $[\text{Mn}_4\text{O}_2\text{L}_5]^+$ , corresponding to the loss of one phosphinate ligand and two core O atoms. Synthesis of the  $^{18}\text{O}$ -isotopomer,  $\text{Mn}_4(^{18}\text{O})_4\text{L}_6$ ,  $^{18}\text{O}$ -**1a**, confirmed these assignments. Negative ion LDI-MS-TOF revealed a single photoproduct corresponding to the phosphinate anion  $\text{L}^-$ . Taken together, the data offer clear evidence for selective photodissociation to form the intact “butterfly complex” **2a**,  $[\text{Mn}_4\text{O}_2\text{L}_5]^+$ .<sup>46</sup>

The yield of the butterfly complex **2a** increased in direct proportion to the laser power, while the ratio of peak intensities for the butterfly/cubane increased by 8-fold and approached a relative quantum yield of 50% at the highest light intensity available without achieving saturation.<sup>20,46</sup> From this, it can be deduced that there is an activation barrier for photoconversion of cubane to butterfly plus oxygen, which can be overcome only upon removal of a phosphinate.

Photoexcitation produced a single species in the 14–200 amu range having a mass of 32 amu for **1a** or 36 amu for  $^{18}\text{O}$ -**1a**.<sup>46</sup> Thus,  $\text{O}_2$  is generated from the corner oxygen atoms of **1a** yielding the butterfly **2a** by intramolecular bond formation, preceded by the release of a phosphinate anion.

By contrast, photoexcitation of **1a** using 532 nm light, corresponding to a d–d ligand field absorption band of the cubane, produced no photochemistry at all; only the parent ion was detected, even though an 8-fold higher intensity was available.<sup>46</sup> Therefore, the photoreaction observed with UV light clearly is photolytic rather than thermal in nature and proceeds only upon weakening the phosphinate binding. Similar results were obtained for the oxidized cubanes **1a**<sup>+</sup> and **1b**<sup>+</sup>.<sup>20,26</sup>

The observation that both **1b** and **1b**<sup>+</sup> produce higher yields of the butterfly photoproduct than do **1a** and **1a**<sup>+</sup>, respectively, means that the presence of the 12 electron-donating methoxy groups on the phenyl rings increases the probability of photodissociation compared with diphenylphosphinate ligands.<sup>26</sup> Thus, electronic induction through the phenyl ring of the ligand is an effective strategy for tuning photochemical reactivity of cubanes. This has been explained on the basis of crystallography<sup>19,39</sup> and DFT calculations of the electron donor ability of the *p*-methoxy groups in **1b**.<sup>26</sup>

## Supporting Environment

The PSII-WOC is encapsulated within a protein structure that holds the metal ions in place and provides for the needed conformational flexibility, chemical inertness to unwanted oxidation, and proton dispersion, while also allowing efficient electrical contact between the cluster and the P680 photoconversion complex. The emulation of these features is likely to be critical to the development of abiological water-oxidizing catalysts.

Two examples of this include the homogeneous catalyst  $[\text{Mn}^{\text{II}}_2(\text{mcbpen})_2(\text{H}_2\text{O})_2]^{2+}$  (mcbpen = *N*-methyl-*N'*-carboxymethyl-bis(2-pyridylmethyl)ethane-1,2-diamine), which employs two tetradentate mcbpen ligands to retard the loss of the Mn centers to solution, facilitating  $\text{O}_2$  evolution for ca. 13 turnovers, using *tert*-butylhydrogen peroxide,<sup>25</sup> and immobilization of  $[(\text{tpy})(\text{H}_2\text{O})\text{Mn}(\mu\text{-O})_2\text{Mn}(\text{H}_2\text{O})(\text{tpy})]^{3+}$  (tpy = terpyridine) within the pores of a clay mineral, facilitating multiple turnovers using  $1\text{e}^-$  oxidants like Ce(IV),<sup>47</sup> with the clay environment thought to facilitate dimer interactions and retard dimer dissociation into monomers.

An alternative approach for catalyst stability and proton conduction is to use a proton-conducting polymer matrix, such as Nafion. Nafion is a fluorinated hydrophobic polymer with ionizable hydrophilic head groups (sulfonic acid). Within Nafion membranes, sulfonic acid or sulfonate groups (for  $\text{Na}^+$  form) generate hydrophilic channels that are ~20 nm wide. These channels are permeable to protons and other cations but not anions.<sup>48</sup> The properties of Nafion have been exploited in many applications, including proton exchange

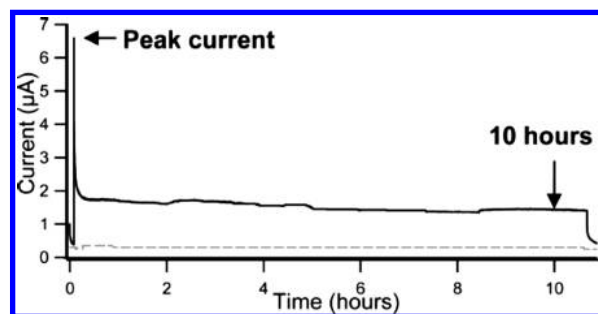


**FIGURE 4.** Photocurrent detected from (black trace) **1b**<sup>+</sup>-Nafion/glassy-C electrode (3 mm diameter) at a potential of 1.00 V vs Ag/AgCl and (gray trace) undoped-Nafion/glassy-C electrode. Electrolyte = aqueous 0.1 M  $\text{Na}_2\text{SO}_4$ . Illumination by a white light source starts at 10 min and ends at 10.5 h.<sup>53</sup>

membranes in various fuel cells and electrolyzers for  $\text{H}_2$  generation<sup>49,50</sup> and Ru water oxidation catalysts.<sup>51</sup>

## A Water-Electrolysis Cell: Redox Coupling to Electrodes

The juxtaposition of hydrophilic and inert hydrophobic domains in Nafion supports the hydrophobic cubane molecules and protects their reactive intermediates, while simultaneously allowing access to water molecules in restricted channels and diffusion of bulk water. Conductive surfaces were coated with Nafion and doped with cubium (**1b**<sup>+</sup>).<sup>52</sup> Immersion of doped membranes in water both provides the reactant and also traps the hydrophobic cubane in the Nafion. Uptake of the intact **1b**<sup>+</sup> into Nafion was proven by UV–vis and EPR spectroscopy<sup>52,53</sup> while voltammetric detection of the redox transition **1b** ↔ **1b**<sup>+</sup> within the cubium/Nafion/glassy carbon electrode indicated that electrochemical contact existed between the catalyst and the electrode.<sup>52</sup> Thus, the **1b**<sup>+</sup>/Nafion/electrode system could be driven electrochemically, removing the need for a chemical oxidant.

When illuminated with light (275–750 nm) and biased at a potential of 1 V vs Ag/AgCl, the **1b**<sup>+</sup>/Nafion/electrode generates a stable photocurrent (Figure 4).<sup>52</sup> Critical tests confirmed water oxidation catalysis by the cubane molecule and that the photocurrent originated only from water (the photocurrent disappeared in acetonitrile).<sup>52,53</sup> The photocurrent was consistently observed with a wide range of electrolytes and for cubane-doped Nafion membranes deposited on a range of conductive surfaces.<sup>52</sup>

The photocurrent increases linearly with increasing solution pH from 2 to 12, as expected for the water oxidation reaction (eq 1). Under illumination at 1 V, cubane-doped Nafion electrodes were shown to release (1)  $\text{O}_2$  gas detected by Clarke electrode and membrane inlet mass spectrometry using  $^{18}\text{O}$ -enriched water and (2) protons in the aqueous phase at 17 times the rate from undoped Nafion/electrodes.



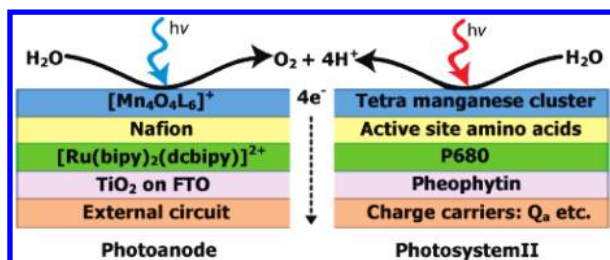


**FIGURE 5.** Schematic showing the conceptual similarity of the photoanode  $1b^+$ -Nafion/ $\text{Ru}(4)$ - $\text{TiO}_2$ , with the PSII-WOC.

The photocurrent from a  $1b^+$ /Nafion/electrode was observed after 65 h of testing.<sup>53</sup> The total quantity of electroactive cubane in the Nafion coating was determined by bulk electrolysis and used to calculate that each cubane molecule is capable of >1000 turnovers without the need for a sacrificial oxidant. This provides a lower limit to the mean light-dependent turnover frequency over this 65 h period to be  $15 \text{ O}_2 \text{ h}^{-1} \text{ cubane}^{-1}$ . This is a lower limit since it is light limited (1 sun), and only a fraction of the reduced catalyst molecules in the  $5 \mu\text{m}$  thick Nafion membrane could diffuse to the electrode for reoxidation during the time interval between photon absorption. This intrinsic rate is  $10^4$ – $10^5$  times slower than light-saturated native PSII-WOC rates in whole cells of microalgae. The mechanism of catalytic turnover has been investigated by EPR, NMR, IR, and UV-vis spectroscopies, and possible reactive intermediates or side products were tentatively identified.<sup>53</sup>

## A Water Photooxidation Cell: Redox Coupling to Light-Driven Electron Transfer

Most recently we have presented evidence showing that the cubium  $1b^+$  doped Nafion system functions as a water oxidation catalyst by coupling to a photoactive dye-sensitized titania film using light as the sole energy source.<sup>54,55</sup> A device based on the dye-sensitized solar cell (DSSC) developed by Graetzel and co-workers<sup>2</sup> was prepared by attaching a ruthenium(II) dye,  $[\text{Ru}^{\text{II}}(\text{bipy})_2(\text{bipy}(\text{COO})_2)]$  (**4**), onto a titania-coated FTO conductive glass anode. This half-cell was overcoated with a Nafion membrane into which  $1b^+$  was introduced by ion-exchange. Figure 5 provides a schematic of this half-cell and compares it to the PSII-WOC. Upon illumination with white light while immersed in aqueous media and attached to a Pt counter electrode, the photoanode released  $\text{O}_2$  gas and protons to solution, simultaneous with photocurrent generation. The complete photoanode represents, in principle, a functional analog of the PSII-WOC that contains the same types of elements, albeit configured in a different and less efficient way (Figure 5). The performance of this device is under investigation and shall be reported elsewhere.

## Conclusions

Through consideration of the key features of catalysis of photosynthetic water oxidation, we have developed a light-activated  $\text{Mn}_4\text{O}_4$ -cubane cluster that catalyzes this reaction *in vitro*. We have coupled this to an electrochemical potential derived from both electrical and photolytic sources to achieve sustained catalytic water oxidation free of the ambiguity caused by use of chemical oxidants. Although significantly different from the natural system in several respects, the key to its success undoubtedly lies in its bioinspired attributes, including (1) cooperation among four electronically coupled Mn ions to activate two substrate water molecules at the corners of a "cubical core", (2) the cubane topology as the most favorable one for lowering the barrier to O–O bond formation and  $\text{O}_2$  release, and (3) the indispensable requirement for aqueous channels and proton removal from the active site for catalytic turnover.

The  $\text{Mn}_4\text{O}_4$ -cubane catalysts recapitulate Nature's principles of photosynthetic water oxidation using only visible light as the energy source. These results validate the bioinspired molecular cluster method for catalysis of water splitting and offer a promising future for solar-powered renewable hydrogen production.

*G.C.D. and G.F.S. thank the Australian Academy of Sciences for travel fellowships; R.B. thanks the Fulbright Foundation for a fellowship. We are most grateful to our coworkers and collaborators whose work we have acknowledged. This research was supported by NIH Grant GM-39932 and an ARC discovery grant.*

## BIOGRAPHICAL INFORMATION

**G. Charles Dismukes** is a member of the Rutgers University faculties in the Departments of Chemistry & Chemical Biology, the Waksman Institute of Microbiology and Biochemistry & Microbiology. His research interests include the chemistry and biology of renewable energy production.

**Robin Brimblecombe** was awarded a Ph.D. in Chemistry by Monash University, Australia, in 2009 and was the recipient of a Fulbright Fellowship to Princeton University, 2007–2008.

**Greg A. N. Felton** was awarded a Ph.D. in Chemistry from the University of Texas at Austin, 2005. Through postdoctoral positions at The University of Arizona and Princeton University, he has pursued his research interests in bioinspired organometallic catalytic systems and electrochemistry.

**Ruslan S. Pryadun** was awarded M.A. and Ph.D. degrees in Chemistry from SUNY at Buffalo. Following postdoctoral appointments at Princeton and Harvard Universities, he joined BASF Corporation.

**John E. Sheats** is Professor Emeritus since 2008 at Rider University and visiting fellow at Princeton University where he works on the synthesis of organometallic catalysts.

**Leone Spiccia** was awarded a Ph.D. from the University of Western Australia. He is currently a Professor of Chemistry at Monash University and is interested in the development of novel photoactive and redox active materials for dye-sensitized solar cells and water splitting devices.

**Gerry Swiegers** is a Fellow at the ARC Centre of Excellence for Electromaterials Science, University of Wollongong. Gerry completed a Ph.D. at the University of Connecticut and carried out postdoctoral work at the Australian National University in Canberra prior to becoming a research group leader at CSIRO, Melbourne.

## REFERENCES

- Bard, A. J.; Fox, M. A. Artificial photosynthesis: Solar splitting of water to hydrogen and oxygen. *Acc. Chem. Res.* **1995**, *28*, 141–145.
- Gratzel, M. Photoelectrochemical cells. *Nature* **2001**, *414*, 338–344.
- Bockris, J. O. M.; Dandapani, B.; Cocke, D.; Ghoroghchian, J. On the splitting of water. *Int. J. Hydrogen Energy* **1985**, *10*, 179–201.
- Dismukes, G. C.; van Willigen, R. T. In *Encyclopedia of Inorganic Chemistry*, 2nd ed.; King, B., Ed.; J. Wiley: Chichester, U.K., 2006; p 6696.
- Lubitz, W.; Reijerse, E. J.; Messinger, J. Solar water-splitting into H<sub>2</sub> and O<sub>2</sub>: Design principles of photosystem II and hydrogenases. *Energy Environ. Sci.* **2008**, *1*, 15–31.
- Barber, J. Crystal structure of the oxygen-evolving complex of photosystem II. *Inorg. Chem.* **2008**, *47*, 1700–1710.
- Ananyev, G. M.; Zaltsman, L.; Vasko, C.; Dismukes, G. C. The inorganic biochemistry of photosynthetic oxygen evolution/water oxidation. *Biochim. Biophys. Acta* **2001**, *1503*, 52–68.
- Carrell, T. G.; Tyryshkin, A. M.; Dismukes, G. C. An evaluation of structural models for the photosynthetic water-oxidizing complex derived from spectroscopic and X-ray diffraction signatures. *J. Biol. Inorg. Chem.* **2002**, *7*, 2–22.
- Yachandra, V. K.; Sauer, K.; Klein, M. P. Manganese cluster in photosynthesis: Where plants oxidize water to dioxygen. *Chem. Rev.* **1996**, *96*, 2927–2950.
- Sauer, K.; Yachandra, V. K. The water-oxidation complex in photosynthesis. *Biochem. Biophys. Acta* **2004**, *1655*, 140–148.
- Yano, J.; Kern, J.; Irrgang, K. D.; Latimer, M. J.; Bergmann, U.; Glatzel, P.; Pushkar, Y.; Biesiadka, J.; Loll, B.; Sauer, K.; Messinger, J.; Zouni, A.; Yachandra, V. K. X-ray damage to the Mn<sub>4</sub>Ca complex in single crystals of photosystem II: A case study for metalloprotein crystallography. *Proc. Natl. Acad. Sci. U.S.A.* **2005**, *102*, 12047–12052.
- Zouni, A.; Witt, H. T.; Kern, J.; Fromme, P.; Krauss, N.; Saenger, W.; Orth, P. Crystal structure of photosystem II from *Synechococcus elongatus* at 3.8 Å resolution. *Nature* **2001**, *409*, 739–743.
- Guskov, A.; Kern, J.; Gabdulkhakov, A.; Broser, M.; Zouni, A.; Saenger, W. Cyanobacterial photosystem II at 2.9-angstrom resolution and the role of quinones, lipids, channels and chloride. *Nat. Struct. Mol. Biol.* **2009**, *16*, 334–342.
- Yano, J.; Kern, J.; Pushkar, Y.; Sauer, K.; Glatzel, P.; Bergmann, U.; Messinger, J.; Zouni, A.; Yachandra, V. K. High-resolution structure of the photosynthetic Mn<sub>4</sub>Ca catalyst from X-ray spectroscopy. *Phil. Trans. R. Soc. B* **2008**, *363*, 1139–1147.
- Ferreira, K. N.; Iverson, T. M.; Maghlaoui, K.; Barber, J.; Iwata, S. Architecture of the photosynthetic oxygen-evolving center. *Science* **2004**, *303*, 1831–1838.
- Sproviero, E. M.; Gascon, J. A.; McEvoy, J. P.; Brudvig, G. W.; Batista, V. S. A model of the oxygen-evolving center of photosystem II predicted by structural refinement based on EXAFS simulations. *J. Am. Chem. Soc.* **2008**, *130*, 6728–6730.
- Vincent, J. B.; Christmas, C.; Chang, H. R.; Li, Q. Y.; Boyd, P. D. W.; Huffman, J. C.; Hendrickson, D. N.; Christou, G. Modeling the photosynthetic water oxidation center: Preparation and properties of tetranuclear manganese complexes containing [Mn<sub>4</sub>O<sub>2</sub>]<sup>6+,7+,8+</sup> cores and the crystal-structures of Mn<sub>4</sub>O<sub>2</sub>(O<sub>2</sub>CMe)<sub>6</sub>(Bipy)<sub>2</sub> and [Mn<sub>4</sub>O<sub>2</sub>(O<sub>2</sub>CMe)<sub>7</sub>(Bipy)<sub>2</sub>](ClO<sub>4</sub>). *J. Am. Chem. Soc.* **1989**, *111*, 2086–2097.
- Carrell, T. G.; Cohen, S.; Dismukes, G. C. Oxidative catalysis by Mn<sub>4</sub>O<sub>4</sub><sup>6+</sup> cubane complexes. *J. Mol. Catal. A: Chem.* **2002**, *187*, 3–15.
- Ruettinger, W. F.; Campana, C.; Dismukes, G. C. Synthesis and characterization of Mn<sub>4</sub>O<sub>4</sub>L<sub>6</sub> complexes with cubane-like core structure: A new class of models of the active site of the photosynthetic water oxidase. *J. Am. Chem. Soc.* **1997**, *119*, 6670–6671.
- Yagi, M.; Wolf, K. V.; Baesjou, P. J.; Bernasek, S. L.; Dismukes, G. C. Selective photoproduction of O<sub>2</sub> from the Mn<sub>4</sub>O<sub>4</sub> cubane core: A structural and functional model for the photosynthetic water-oxidizing complex. *Angew. Chem., Int. Ed.* **2001**, *40*, 2925–2928.
- Yu, Y.; Dubey, M.; Bernasek, S. L.; Dismukes, G. C. Self-assembled monolayer of organic iodine on a Au surface for attachment of redox-active metal clusters. *Langmuir* **2007**, *23*, 8257–8263.
- Mishra, A.; Wernsdorfer, W.; Abboud, K. A.; Christou, G. The first high oxidation state manganese-calcium cluster: relevance to the water oxidizing complex of photosynthesis. *Chem. Commun.* **2005**, *1*, 54–56.
- Messinger, J. Evaluation of different mechanistic proposals for water oxidation in photosynthesis on the basis of Mn<sub>4</sub>O<sub>4</sub>Ca structures for the catalytic site and spectroscopic data. *Phys. Chem. Chem. Phys.* **2004**, *6*, 4764–4771.
- Dasgupta, J.; Ananyev, G. M.; Dismukes, G. C. Photoassembly of the water-oxidizing complex in photosystem II. *Coord. Chem. Rev.* **2008**, *252*, 347–360.
- Poulsen, A. K.; Rompel, A.; McKenzie, C. J. Water oxidation catalyzed by a dinuclear Mn complex: A functional model for the oxygen-evolving center of photosystem II. *Angew. Chem., Int. Ed.* **2005**, *44*, 6916–6920.
- Wu, J.-Z.; Angelis, F. D.; Carrell, T. G.; Yap, G. P. A.; Sheats, J.; Car, R.; Dismukes, G. C. Tuning the photo-induced O<sub>2</sub>-evolving reactivity of Mn<sub>4</sub>O<sub>4</sub><sup>6+</sup> and Mn<sub>4</sub>O<sub>4</sub><sup>7+</sup> manganese-oxo cubane complexes. *Inorg. Chem.* **2006**, *45*, 189–195.
- Haumann, M.; Liebisch, P.; Muller, C.; Barra, M.; Grabolle, M.; Dau, H. Photosynthetic O<sub>2</sub> formation tracked by time-resolved X-ray experiments. *Science* **2005**, *310*, 1019–1021.
- Kulik, L. V.; Epel, B.; Lubitz, W.; Messinger, J. Electronic structure of the Mn<sub>4</sub>O<sub>4</sub>Ca cluster in the S<sub>0</sub> and S<sub>2</sub> states of the oxygen-evolving complex of photosystem II based on pulse Mn55-ENDOR and EPR spectroscopy. *J. Am. Chem. Soc.* **2007**, *129*, 13421–13435.
- Kuzek, D.; Pace, R. J. Probing the Mn oxidation states in the OEC. Insights from spectroscopic, computational and kinetic data. *Biochim. Biophys. Acta* **2001**, *1503*, 123–137.
- Rappaport, F.; Guergova-Kuras, M.; Nixon, P. J.; Diner, B. A.; Lavergne, J. Kinetics and pathways of charge recombination in photosystem II. *Biochemistry* **2002**, *41*, 8518–8527.
- Manchanda, R.; Brudvig, G. W.; Crabtree, R. H. High-valent oxomanganese clusters - Structural and mechanistic work relevant to the oxygen-evolving center in photosystem-II. *Coord. Chem. Rev.* **1995**, *144*, 1–38.
- Brimblecombe, R.; Bond, A. M.; Dismukes, G. C.; Swiegers, G. F.; Spiccia, L. Electrochemical investigation of Mn<sub>4</sub>O<sub>4</sub>-cubane water-oxidizing clusters. *Phys. Chem. Chem. Phys.* **2009**, *11*, 6441–6449.
- Ruettinger, W. F.; Ho, D. M.; Dismukes, G. C. Protonation and dehydration reactions of the Mn<sub>4</sub>O<sub>4</sub>L<sub>6</sub> cubane and synthesis and crystal structure of the oxidized cubane [Mn<sub>4</sub>O<sub>4</sub>L<sub>6</sub>]<sup>+</sup>: A model for the photosynthetic water oxidizing complex. *Inorg. Chem.* **1999**, *38*, 1036–1037.
- Petrie, S.; Stranger, R.; Pace, R. L. Structural, magnetic coupling and oxidation state trends in models of the CaMn<sub>4</sub> cluster in photosystem II. *Chem.—Eur. J.* **2008**, *14*, 5482–5494.
- Westphal, K. L.; Tommos, C.; Cukier, R. I.; Babcock, G. T. Concerted hydrogen-atom abstraction in photosynthetic water oxidation. *Curr. Opin. Plant Biol.* **2000**, *3*, 236–242.
- Dasgupta, J.; van Willigen, R. T.; Dismukes, G. C. Consequences of structural and biophysical studies for the molecular mechanism of photosynthetic oxygen evolution: Functional roles for calcium and bicarbonate. *Phys. Chem. Chem. Phys.* **2004**, *6*, 4793–4802.
- Carrell, T. G.; Bourles, E.; Lin, M.; Dismukes, G. C. Transition from hydrogen atom to hydride abstraction by [Mn<sub>4</sub>O<sub>4</sub>(O<sub>2</sub>PPh<sub>2</sub>)<sub>6</sub>] versus [Mn<sub>4</sub>O<sub>4</sub>(O<sub>2</sub>PPh<sub>2</sub>)<sub>6</sub>]<sup>+</sup>: O-H bond dissociation energies and the formation of [Mn<sub>4</sub>O<sub>3</sub>(OH)(O<sub>2</sub>PPh<sub>2</sub>)<sub>6</sub>]. *Inorg. Chem.* **2003**, *42*, 2849–2858.
- Maneiro, M.; Ruettinger, W. F.; Bourles, E.; McLendon, G. L.; Dismukes, G. C. Kinetic of proton-coupled electron-transfer reactions to the manganese-oxo “cubane” complexes containing the Mn<sub>4</sub>O<sub>4</sub><sup>6+</sup> and Mn<sub>4</sub>O<sub>4</sub><sup>7+</sup> core types. *Proc. Natl. Acad. Sci. U.S.A.* **2003**, *100*, 3707–3712.
- Wu, J. Z.; Sellitto, E.; Yap, G. P. A.; Sheats, J.; Dismukes, G. C. Trapping an elusive intermediate in manganese-oxo cubane chemistry. *Inorg. Chem.* **2004**, *43*, 5795–5797.
- Bordwell, F. G.; Harrelson, J. A.; Zhang, X. M. Homolytic bond-dissociation energies of acidic C-H bonds activated by one or two electron-acceptors. *J. Org. Chem.* **1991**, *56*, 4448–4450.
- Handoo, K. L.; Cheng, J. P.; Parker, V. D. Hydride affinities of organic radicals in solution - a comparison of free-radicals and carbenium ions as hydride ion acceptors. *J. Am. Chem. Soc.* **1993**, *115*, 5067–5072.
- Gardner, K. A.; Kuehnert, L. L.; Mayer, J. M. Hydrogen atom abstraction by permanganate: Oxidations of arylalkanes in organic solvents. *Inorg. Chem.* **1997**, *36*, 2069–2078.



- 43 Lubitz, W.; Reijerse, E. J.; Messinger, J. Solar water-splitting into H<sub>2</sub> and O<sub>2</sub>: Design principles of photosystem II and hydrogenases. *Energy Environ. Sci.* **2008**, *1*, 15–31.
- 44 Tyryshkin, A. M.; Watt, R. K.; Baranov, S. V.; Dasgupta, J.; Hendrich, M. P.; Dismukes, G. C. Spectroscopic evidence for Ca<sup>2+</sup> involvement in the assembly of the Mn<sub>4</sub>Ca cluster in the photosynthetic water-oxidizing complex. *Biochemistry* **2006**, *45*, 12876–12889.
- 45 Brudvig, G. W. Water oxidation chemistry of photosystem II. *Philos. Trans. R. Soc. B* **2008**, *363*, 1211–1219.
- 46 Ruettinger, W.; Yagi, M.; Wolf, K.; Bernasek, S.; Dismukes, G. C. O<sub>2</sub> evolution from the manganese-oxo cubane core Mn<sub>4</sub>O<sub>4</sub><sup>6+</sup>: A molecular mimic of the photosynthetic water oxidation enzyme. *J. Am. Chem. Soc.* **2000**, *122*, 10353–10357.
- 47 Narita, K.; Kuwabara, T.; Sone, K.; Shimizu, K. i.; Yagi, M. Characterization and activity analysis of catalytic water oxidation induced by hybridization of [(OH<sub>2</sub>)(terpy)Mn(μ-O)<sub>2</sub>Mn(terpy)(OH<sub>2</sub>)]<sup>3+</sup> and clay compounds. *J. Phys. Chem. B* **2006**, *110*, 23107–23114.
- 48 Blake, N. P.; Petersen, M. K.; Voth, G. A.; Metiu, H. Structure of hydrated Na-Nafion polymer membranes. *J. Phys. Chem. B* **2005**, *109*, 24244–24253.
- 49 Zhu, J.; Sattler, R.; Garsuch, A.; Yezep, O.; Pickup, P. Optimisation of polypyrrole/Nafion composite membranes for direct methanol fuel cells. *Electrochim. Acta* **2006**, *51*, 4052–4060.
- 50 Park, H.; Choi, W. Visible-light-sensitized production of hydrogen using perfluorosulfonate polymer-coated TiO<sub>2</sub> nanoparticles: An alternative approach to sensitizer anchoring. *Langmuir* **2006**, *22*, 2906–2911.
- 51 Yagi, M.; Kentaro Nagoshi, M. K. Cooperative catalysis and critical decomposition distances between molecular water oxidation catalysts incorporated in a polymer membrane. *J. Phys. Chem. B* **1997**, *101*, 5143–5146.
- 52 Brimblecombe, R.; Swiegers, G. F.; Dismukes, G. C.; Spiccia, L. Sustained water oxidation photocatalysis by a bioinspired manganese cluster. *Angew. Chem., Int. Ed.* **2008**, *120*, 7445–7448.
- 53 Brimblecombe, R.; Kolling, D. R. J.; Bond, A. M.; Dismukes, G. C.; Swiegers, G. F.; Spiccia, L. Sustained water oxidation by [Mn<sub>4</sub>O<sub>4</sub>]<sup>7+</sup> core complexes inspired by oxygenic photosynthesis. *Inorg. Chem.* **2009**, *48*, 7269–7279.
- 54 Dismukes, G. C.; Brimblecombe, R.; Koo, A.; Swiegers, G. F.; Spiccia, L. Inorganic chemistry in service of renewable energy science: Solar driven water oxidation by bioinspired manganese catalysts. *Abstracts of Papers, 238th ACS National Meeting*; American Chemical Society: Washington, DC, 2009; Abstract INOR 709.
- 55 Service, R. A. New trick for splitting water with sunlight. *Science* **2009**, *325*, 1200–1201.